Available online at www.academicpaper.org
Academic @ Paper

International Journal of Energy Applications and Technologies
Vol. 3, Issue 2, pp. 41 – 49, 2016

www.academicpaper.org/index.php/IJEAT

Research Article

HEAT TRANSFER OF TWO PHASES (WATER – AIR) IN HORIZONTAL SMOOTH AND RIBBED DUCTS

Riyadh S. Al-Turaihi*, Sarah Hasan Oleiwi*

*College of Engineering, Dept. of Mech. Eng., Babylon University

Received 2nd November 2016, Accepted 6th November 2016

Abstract

Computational fluid dynamics (CFD) was used to investigate the flow of water and air in smooth and ribbed duct. Temperature was applied for the top and the bottom of the duct where the ribs are located. The heat transfer coefficient were calculate at different location inside the ducts and the results was validated using several heat transfer coefficient correlations that was developed by other researchers. Three shapes of ribs was studied which are rectangular, trapezoidal, and triangle. Three water velocities and three air velocities was studied (0.4, 0.6, and 0.8 m/s), and (0.12, 0.15, and 0.18 m/s), respectively. The heat transfer coefficient increased by adding ribs, it also increased as the velocity of the flow increased.

Keywords- *Heat transfer, Ribbed duct, Two phase, Ansys Fluent, CFD.*

1. Introduction

There are two types of techniques available to increase the heat transfer which are active and passive techniques. Passive techniques include additives of fluid, devices of swirl flow, extended and coated surfaces, and roughed surfaces anything that include applying special surface geometry. Active techniques include vibration of surface, acoustic or electric fields, and mechanical aids simply the techniques that requisite external power source [11]. Ducts and pipes that roughed with ribs are widely used in several applications such as ventilation, turbine blades, and heat exchangers [1]. Ribbed ducts are commonly used for the enhancement of convection heat transfer since the presence of ribs increase the turbulent and produce flow circulation which increase the heat and mass transfer also the thermal boundary layer thickness are reduced by the ribs due to the secondary flow regions that appear near the wall which increase the heat transfer rate [2,10]. Several researcher studied the ribbed channels, Song et al. [17], compared the trajectories and particle velocities and particle impacts wall wastage by means of rib and smooth welding wall, experimentally and computationally. Both results showed that wall erosion are reduced by adding ribs on wall. Manca et al. [11], numerically investigated the angle between the ribbed surface and the direction of the fluid flow using three dimensional rectangular ribbed channel model. Ansari and Arzandi [2], experimentally investigated the air water two phase flow using ducts that are smooth and ribbed to show the effect of ribs height on the boundaries, they also presented a flow map diagram. Yemenici and Sakin [18], used the finite volume method to investigate the flow of air over heated ribbed wall, they showed that heat transfer are improved by the presence of ribs. Coletti et al. [5], used the particle image velocimetry two dimensional time resolved to study the turbulent flow within a rotating channel having ribs along one wall. They showed that both the centrifugal force and Coriolis force effects the fluid dynamics as the ribbed wall is heated. Boukadoum and Benzaoui [3], performed a computational fluids dynamics simulation to analyze the flow and to study the convection heat transfer in solar air heaters duct having rectangular ribs. Komeil et al. [10], numerically investigated the ribbed tubes convection heat transfer using Al_2O_3-water nonofluid turbulent flow and different shapes of rib. They showed that it's thermodynamically advantageous. Jaiswal S. and Aharwal [7], performed three dimensional numerical study using Ansys fluent to study the fluid flow characteristics and the heat transfer with in ribbed

* Corresponding Authors;
drriyadhalturaihi@yahoo.com
sarah.ha369@gmail.com

Note: This paper has been presented at the International Conference on Advanced Technology & Sciences (ICAT'16) held in Konya (Turkey).

channel. In this work a computational fluid dynamics simulation was performed for a two phase (air-water) flow in ribbed channel. Three rib shapes was used (Rectangular, Trapezoidal, and Triangle) and the results compared with smooth channel to show the effect of ribs on the heat transfer coefficient. The results of the CFD two phase model was validated using heat transfer coefficients correlations that developed by Boyko and Kruzhilin [4], Serizawa and Michiyoshi [15], and Kim and Ghajar [8]. And the results were in good agreement.

2. Problem Description

Ribbed duct with two phase (air – water) flow flowing through it was investigated, figure 1a. Two dimensional geometry model was generated using SolidWorks 2013. The duct consists of a (146 cm) entrance section to insure a fully developed flow and (54 cm) ribbed heated section with (4.5 cm) height. Uniform temperature was applied on the top and bottom of the ribbed section. The inlet of air and water was given a special arrangement, detailed view of the inlet section are shown in figure 1b.Three different shapes of ribs was studied which as (rectangular, trapezoidal, and triangle) as shown in figure 2, smooth duct was also generated to show the difference made by the ribs. The ribs have a base width of (w = 1.5 cm) and height of (e = 0.8 cm) along with a bitch distance of (b = 4.5 cm). Three values of air and water velocities was investigated (0.12, 0.15, and 0.18 m/s), and (0.4, 0.6, and 0.8 m/s), respectively. Table 1 shows the tests that was performed with respect to the water and air velocities for each rib shape and for the smooth duct as well. Ansys Fluent 15.0 was used to simulate the flow of air water in a ribbed duct. Two phase mixture model along with the k-epsilon standard turbulent model were used using water as the primary phase and air as the secondary phase.

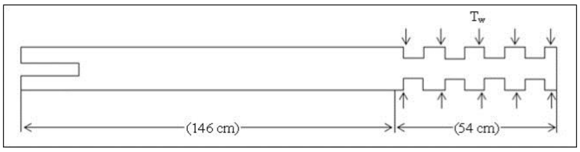

(a)

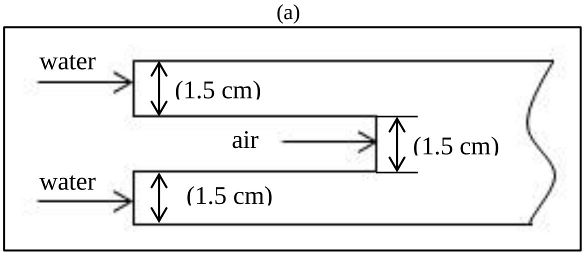

(b)

Fig. 1. Problem description (a) The rectangular ribbed duct (b) The inlet section.

2.1. Mesh

Quadrilateral unstructured mesh was performed for the models using Ansys 15.0, the number of elements were (240121, 239009, 243329, and 245875) for rectangular ribbed, trapezoidal ribbed, triangle ribbed, and smooth duct. Three mesh sizes were used to check the mesh dependence and the accuracy of the results. Table 2 shows the number of element for the mesh sizes used. The percentage deviation of the heat transfer coefficient results with several heat transfer correlations are shown as well in table 2, for smooth duct. Figure 3 shows the initial mesh for two types of ribs.

Table 1. The tests with respect to water-air velocities.

Test number	Water velocity (m/s)	Air velocity (m/s)
Test 1	0.4	0.12
Test 2	0.4	0.15
Test 3	0.4	0.18
Test 4	0.6	0.12
Test 5	0.6	0.15
Test 6	0.6	0.18
Test 7	0.8	0.12
Test 8	0.8	0.15
Test 9	0.8	0.18

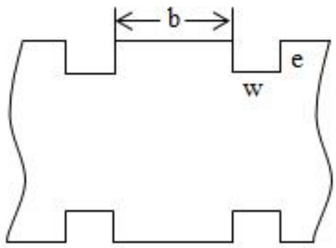

(a) Rectangular

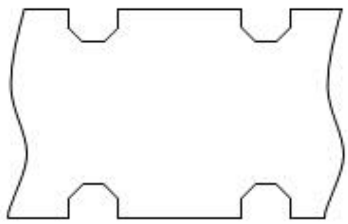

(b) Trapezoidal

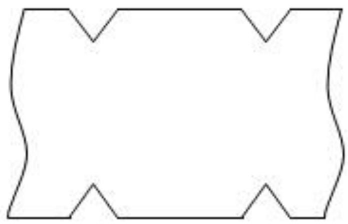

(c) Triangle

Fig. 2. Ribs shape.

2.2. Boundary conditions

Boundary conditions used for this model are:

I. *Inlet Velocity, which is set as*

U_x = inlet velocity, U_y =0, T_{in}=288 K

$\frac{\partial}{\partial x}(U_x) = 0$, $\frac{\partial}{\partial x}(U_y) = 0$

II. *Wall: Wall temperature on the ribbed section equal to 322 K was set*

T_w=322 K

III. *Outlet: The outlet of the duct was set as an outlet pressure*

P=0, T_{out}=288 K

Table 2. Mesh validation

Number of element	3540	109349	245875
(h %) with Boyko and Kruzhilin corr.	24.96 %	16.36 %	7.04 %
(h %) with Serizawa and Michiyoshi corr.	26.62 %	18.62 %	6.5 %
(h %) with Shah corr.	28.03 %	21.06 %	2.71 %
(h %) with Kim and Ghajar corr.	39.89 %	32.87 %	18.85 %

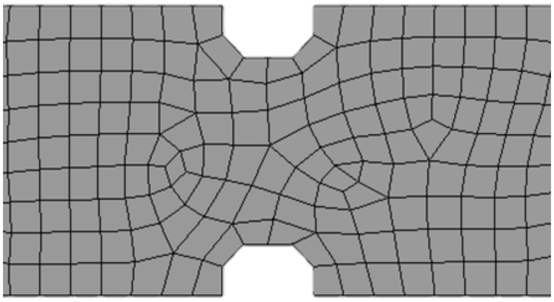

(a) Trapezoidal ribbed duct.

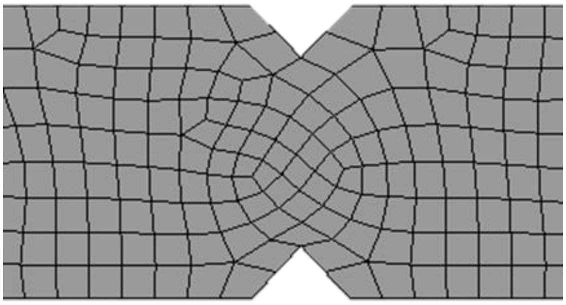

(b) Triangle ribbed duct

Fig. 3. Initial mesh.

2.3. Governing equations for the models used

The mixture model is used in this work to represent the flow of water and air in the ribbed duct. This model is used when the phases of a multiphase flow move at different velocities. The mixture model solves the equation of continuity, momentum and energy for mixture [6].

I. *Continuity Equation*

The equation general form is as (1)

$$\frac{\partial}{\partial t}(\rho_m) + \nabla.(\rho_m \vec{u}_m) = 0 \quad \text{............. (1)}$$

Where $\vec{u}_m$ and ρ_m is the mass-averaged velocity and the mixture density, respectively, represented as (2) and (3)

$$\vec{u}_m = \frac{\sum_{k=1}^{n} \alpha_k \rho_k \vec{u_k}}{\rho_m} \quad \text{............. (2)}$$

$$\rho_m = \sum_{k=1}^{n} \alpha_k \rho_k \quad \text{............. (3)}$$

α_k is the volume fraction of phase k.

II. *Momentum equation*

The equation general form is as (4)

$$\frac{\partial}{\partial t}(\rho_m \vec{u}_m) + \nabla.(\rho_m \vec{u}_m \vec{u}_m) = -\nabla p + \nabla.[\mu_m(\nabla \vec{u}_m + \nabla \vec{u}_m^T)] + \rho_m \vec{g}$$
$$+\vec{F} + \nabla.(\sum_{k=1}^{n} \alpha_k \rho_k \vec{u}_{dr,k} \vec{u}_{dr,k}) \quad \text{.............. (4)}$$

Where n is the number of phases

F is a body force, μ_m is the viscosity of the mixture represented as (5), and $\vec{u}_{dr,k}$ is the drift velocity for secondary phase k represented as (6):

$$\mu_m = \sum_{k=1}^{n} \alpha_k \mu_k \quad \text{.............. (5)}$$

$$\vec{u}_{dr,k} = \vec{u}_k - \vec{u}_m \quad \text{............. (6)}$$

III. *Energy equation*

The equation general form is as (7)

$$\frac{\partial}{\partial t}\sum_{k=1}^{n}(\alpha_k \rho_k E_k) + \nabla.\sum_{k=1}^{n}(\alpha_k \vec{u}_k(\rho_k E_k + p)) = \nabla.(k_{eef} \nabla T) + S_E \quad \text{.............. (7)}$$

Where S_E includes any other volumetric heat sources, k_{eef} is the effective conductivity, and E_k represented as (8) for compressible phase or equal to h_k for incompressible phase.

$$E_k = h_k - \frac{p}{\rho_k} + \frac{u_k^2}{2} \quad \text{.............. (8)}$$

IV. *Turbulence model*

The turbulent model used for this computational study is k-epsilon standard mixture model. The equations general form for this model is as (9a,b).

$$\frac{\partial}{\partial t}(\rho_m k) + \nabla.(\rho_m \vec{v}_m k) = \nabla.\left(\frac{\mu_{t,m}}{\sigma k}\nabla k\right) + G_{k,m} - \rho_m \in \quad \text{.............. (9a)}$$

$$\frac{\partial}{\partial t}(\rho_m \in) + \nabla.(\rho_m \vec{v}_m \in) = \nabla.\left(\frac{\mu_{t,m}}{\sigma_\in}\nabla \in\right) + \frac{\in}{k}(C_{1\in} G_{k,m} - C_{2\in}\rho_m \in \quad \text{.............. (9b)}$$

Where k is the Momentum exchange coefficient, ϵ is the turbulent dissipation rate (m^2/s^3), and σ is the Surface tension (kg/m).

3. Results Validation

The heat transfer coefficient results of the simulated model in this work was validated using the two phase heat transfer coefficient correlations that was developed by other researchers. The researcher are

Boyko and Kruzhilin [4], Serizawa and Michiyoshi [15], Shah and Kim and Ghajar [9]. The correlations formulas are as follows.

I. Boyko and Kruzhilin [4]

Developed a correlation to calculate the heat transfer coefficient for two phase in horizontal tube. They used the correlation to calculate the heat transfer coefficient through the condensation of steam for horizontal tube, they validated their correlation using experimental results.

$$h_{TP} = h_L \left(1 + x\left(\frac{\rho_L}{\rho_G} - 1\right)\right)^{0.5} \quad \text{.............. (10)}$$

Where the liquid heat transfer coefficient evaluated as (11):

$$h_L = 0.021 \mathrm{Re}_L^{0.8} \mathrm{Pr}_L^{0.43}\left(\frac{k_L}{D}\right) \quad \text{.............. (11)}$$

II. Serizawa, Kataoka, and Michiyoshi, [15]

Developed an empirical correlation to calculate the diffusivity ratio of the two phase (air - water) heat transfer coefficient to the single phase (water) heat transfer coefficient. The correlation, eq. (12), was used in this paper to calculate the two phase heat transfer coefficient, the single phase heat transfer coefficient are evaluated from Sieder and Tate [16], eq. (13).

$$\frac{h_{TP}}{h_L} = 1 + 462 X_{TT}^{-1.27} \quad \text{.............. (12)}$$

$$Nu_L = 0.027 \mathrm{Re}_L^{0.8} \mathrm{Pr}_L^{0.33}\left(\frac{\mu_B}{\mu_W}\right)^{0.14} \quad \text{.............. (13)}$$

Where X_{TT} is the Martinelli parameter, and x is the flow quality, evaluated as (14, and 15), respectively.

$$X_{TT} = \left(\frac{1-x}{x}\right)^{0.9}\left(\frac{\rho_G}{\rho_L}\right)^{0.5}\left(\frac{\mu_L}{\mu_G}\right)^{0.1} \quad \text{.............. (14)}$$

$$x = \frac{\dot{m}_G}{\dot{m}_G + \dot{m}_L} \quad \text{.............. (15)}$$

III. Shah M. M.

Developed a correlation for horizontal and vertical ducts to calculate the two phase (water - air) heat transfer coefficient.

$$\frac{h_{TP}}{h_L} = \left(1 + \frac{u_G}{u_L}\right)^{1/4} \quad \text{.............. (16)}$$

Where h_L is evaluated as (17).

$$Nu_L = 0.023 \mathrm{Re}_L^{0.8} \mathrm{Pr}_L^{0.4}\left(\frac{\mu_B}{\mu_W}\right)^{0.14} \quad \text{.............. (17)}$$

IV. Kim D. and Ghajar A. J. [9]

Developed a heat transfer correlation for two phase (air - water) flow, the correlation are developed based on vertical pipes and different patterns experiments data. They modified the correlation to calculate the two phase heat transfer coefficient for horizontal pipes with good accuracy, eq. (18). Liquid phase heat transfer coefficient was evaluated using Dittus and Boelter heat transfer correlation (19).

$$\frac{h_{TP}}{(1-\alpha)h_L} = \left[1 + 0.27\left(\frac{x}{1-x}\right)^{-0.04}\left(\frac{\alpha}{1-\alpha}\right)^{1.21}\left(\frac{\mathrm{Pr}_G}{\mathrm{Pr}_L}\right)^{0.66}\left(\frac{\mu_G}{\mu_L}\right)^{-0.72}\right] \quad \text{.............. (18)}$$

$$Nu_L = 0.0243 \mathrm{Re}_L^{0.8} \mathrm{Pr}_L^{0.4} \quad \text{.............. (19)}$$

Where x is the flow quality, and α is the void fraction evaluated as (15) and (20), respectively.

$$\alpha = \left[1 + \left(\frac{u_G}{u_L}\right)\left(\frac{1-x}{x}\right)\frac{\rho_G}{\rho_L}\right]^{-1} \quad \text{.............. (20)}$$

The deviation percentage between the results is (7.04%, 6.5%, 2.71%, and 18.85%), respectively, as shown in figure 4. These correlations were compared with smooth duct since it was correlated based on smooth ducts and pipes experiments data.

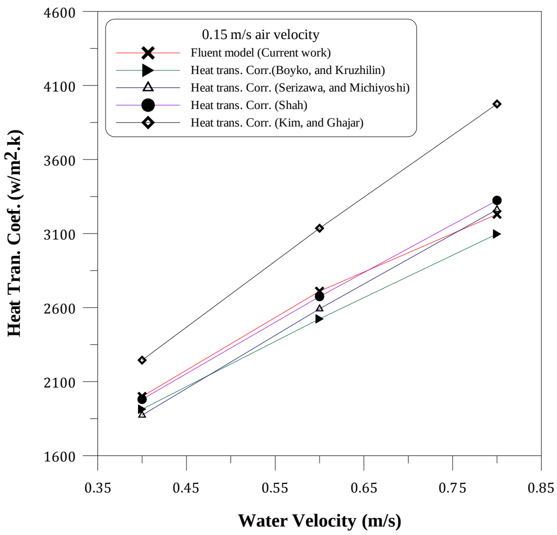

Fig. 4. Comparison between the heat transfer coefficient of the current work and the correlation developed by [4,9,15]. 0.15 m/s air velocity and different water velocities.

4. Results and Discussions

Two phase (water-air) flow through rectangular duct that roughed with different shapes ribs (rectangular, trapezoidal, triangle) was investigated using Ansys Fluent 15.0. three values of water and air velocities was studies. Figure 5 shows the local heat transfer coefficient for the duct for smooth and ribbed ducts, for several values of air and water velocities, the trend of the heat transfer coefficient is the same. In the smooth duct the values of the heat transfer coefficient is the same, as for the ribbed duct the value of the heat transfer coefficient are increased also a complex shape are appear, an amplitude are appear periodically. Figure 6 shows the local heat transfer coefficient for rectangular ribbed duct and smooth duct, this figure shows that the amplitude appear at a certain location which is the where the ribs are located. At ribs and the leading edge of the ribs the velocity is increased which increase the heat transfer coefficient, at the trailing edge the velocity are lower which give low value of the heat transfer coefficient. Figure 7 shows the average heat transfer coefficient for the three shapes of ribs with respect to the water velocity and at different values of the air velocity, as it seems the heat transfer coefficient increase as the value of water velocity increase. The same effect are appear as the value of air velocity increase but with less percentage increase as shown in figure 8. Increasing the velocity will increase the turbulence produced in the duct and the flow mixing will increase as well due to the presence of ribs inside the duct which conversely will increase the heat transfer coefficient. Figure 9 shows the Reynolds number effect on the average value of the heat transfer for smooth and ribbed ducts, as the Reynolds number increase the heat transfer increase for both smooth and ribbed ducts but the percentage increase are not the same, ribbed ducts have more heat transfer areas which mean more heat to be translated in to the duct. Heat transfer coefficient for rectangular ribbed duct increased by (73.97%), as for the trapezoidal ribbed duct increased by (99.14%), where the triangle ribbed duct increased by (135.65%). Figure 10, 11, 12 shows the distribution of water and air inside the ducts for the three different shape ribs. The trailing edge of the ribs are place where eddy are formed and recirculation appear. As the velocity of water and air increased the circulation of flow in the duct increase. Figure 13 shows close view for the flow distribution across the rib, the flow at the leading edge of the rib have high velocity whereas at the rib the flow are separated and reattached after the trailing edge. At the trailing edge of the rib the eddy are formed and flow circulation appear. The area for the leading edge and the trailing edge behavior are at its biggest value for the rectangular ribs and at its smallest value for the triangle ribs. Figure 14 shows the temperature distribution for the three ribbed ducts, this figure shows the temperature are at its higher value at the tailing edge of the ribs and for the three ribs shapes.

5. Conclusions

In this paper the two phase heat transfer coefficient for ribbed and smooth ducts was investigated using Ansys Fluent 15.0 computational fluid dynamics. The coefficient of the ribbed ducts was compared with the smooth duct and found to be increased by 73.97 % for rectangular ribbed duct, 99.14 % for trapezoidal ribbed duct, and 135.65 % for triangle ribbed duct. It also found that the heat transfer coefficient increase as the velocity of the flow increase. The distribution of the water and air in the duct was shown as well as the temperature distribution, eddy was shown to be formed at the trailing edge of the ribs and the temperature found to be at its higher value at the trailing edge of the ribs and for the three types of ribs.

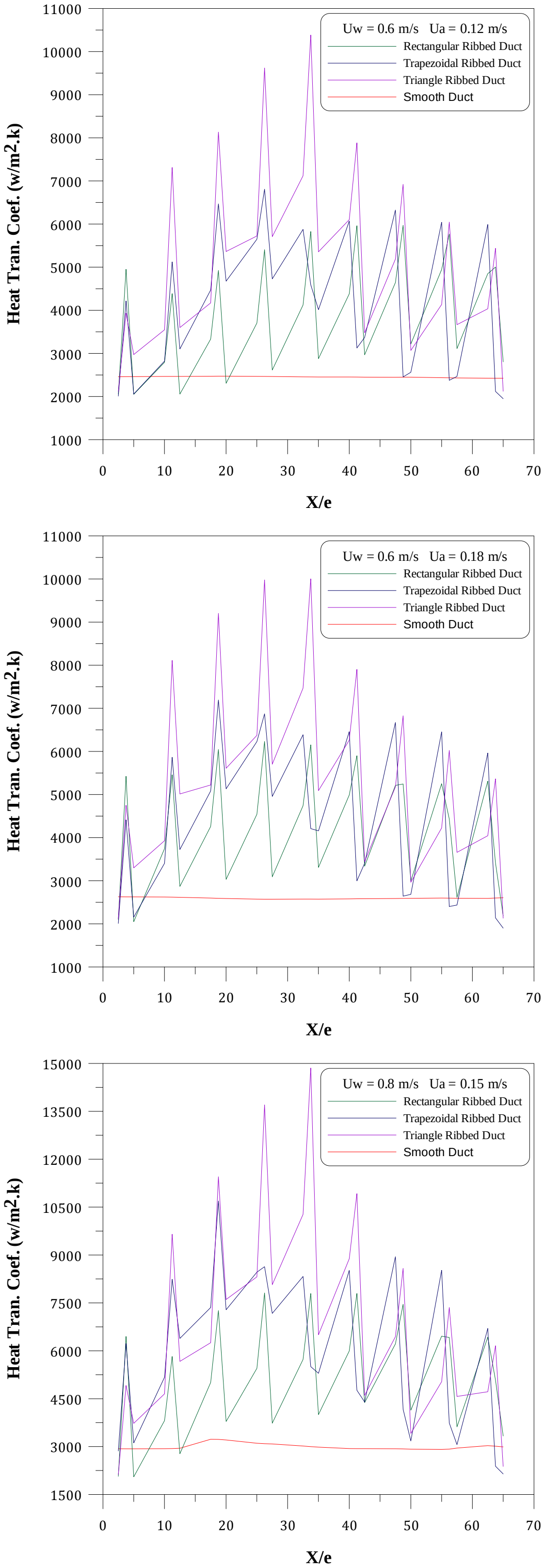

Fig. 5. Effect of ribs on the local heat transfer coefficient at different values of air and water velocities.

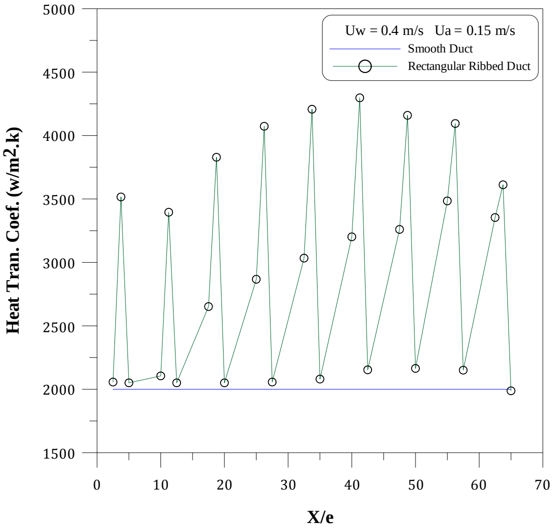

Fig. 6. Local heat transfer for smooth and rectangular ribbed ducts.

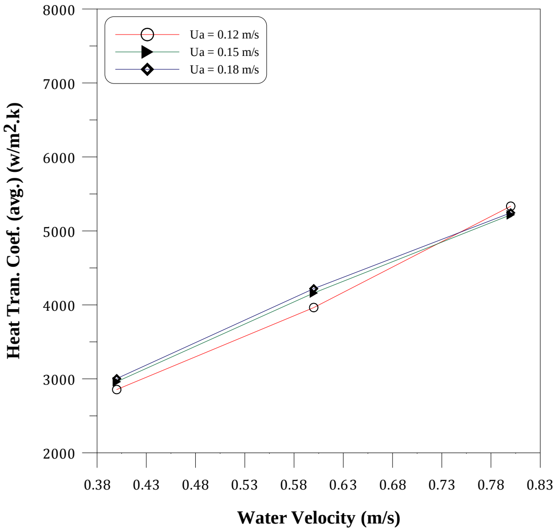

(a) Rectangular ribbed duct.

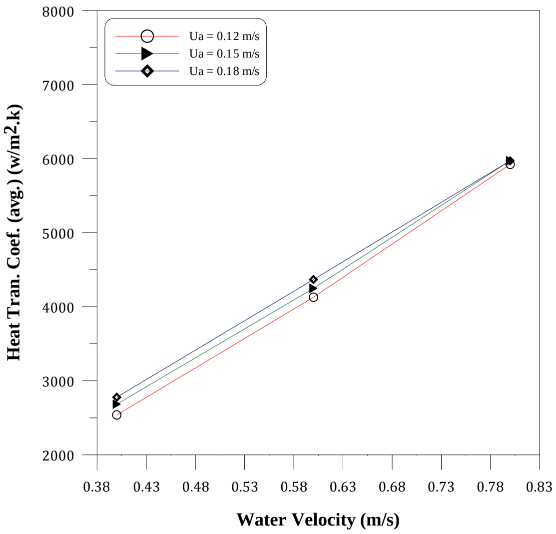

(b) Trapezoidal ribbed duct.

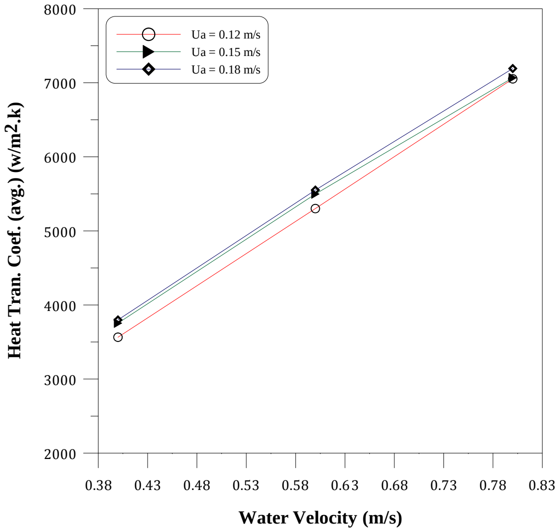

(c) Triangle ribbed duct.

Fig. 7. Effect of water velocity on the average heat transfer coefficient at different air velocities.

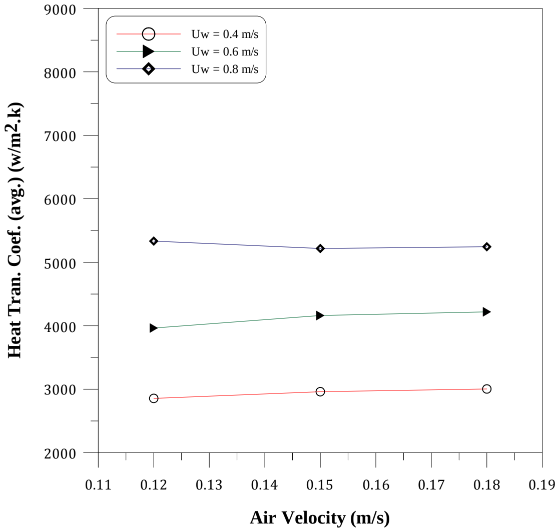

(a) Rectangular ribbed duct.

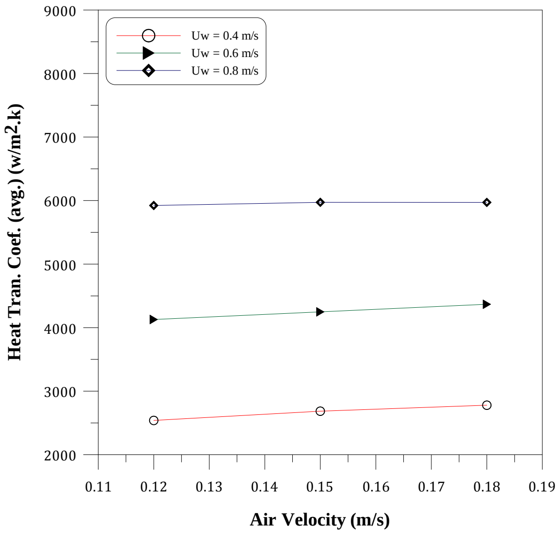

(b) Trapezoidal ribbed duct.

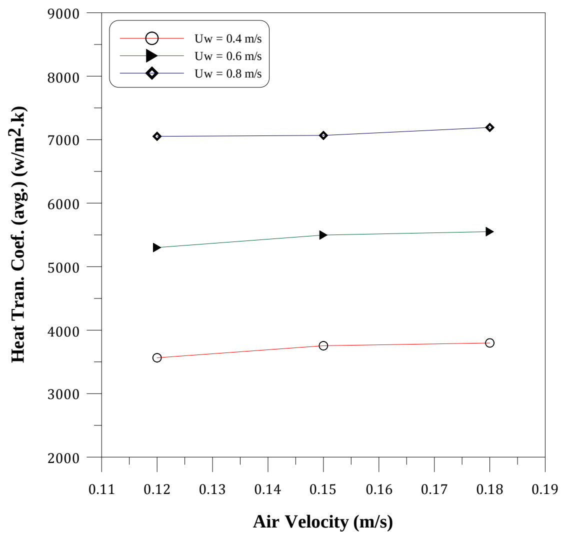

(c) Triangle ribbed duct

Fig. 8. Effect of air velocity on the average heat transfer coefficient at different water velocities.

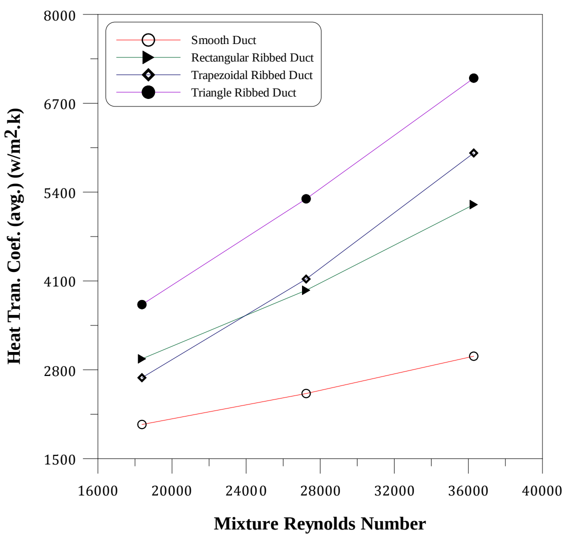

Fig. 9. Effect of Reynolds number on the average heat transfer coefficient for smooth and ribbed duct.

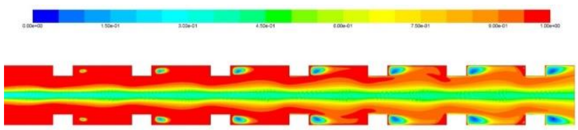

(a)

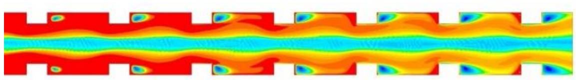

(b)

Fig. 10. Rectangular ribbed duct (a) 0.4 m/s water velocity and 0.18 m/s air velocity (b) 0.8 m/s water velocity and 0.18 m/s air velocity.

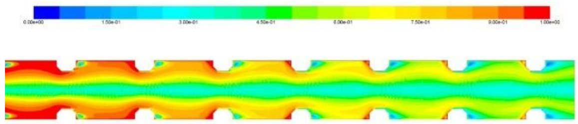

(a)

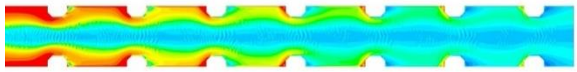

(b)

Fig. 11. Trapezoidal ribbed duct at (a) 0.4 m/s water velocity and 0.18 m/s air velocity (b) 0.8 m/s water velocity and 0.18 m/s air velocity.

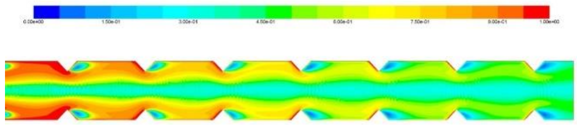

(a)

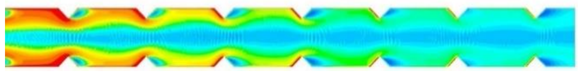

(b)

Fig. 12. Triangle ribbed duct at (a) 0.4 m/s water velocity and 0.18 m/s air velocity (b) 0.8 m/s water velocity and 0.18 m/s air velocity.

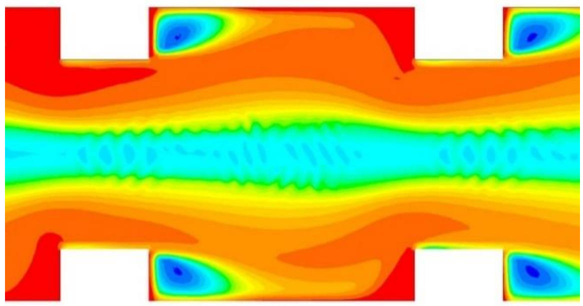

(a) Rectangular ribbed duct.

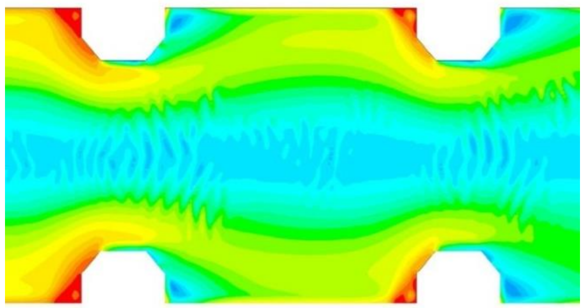

(b) Trapezoidal ribbed duct.

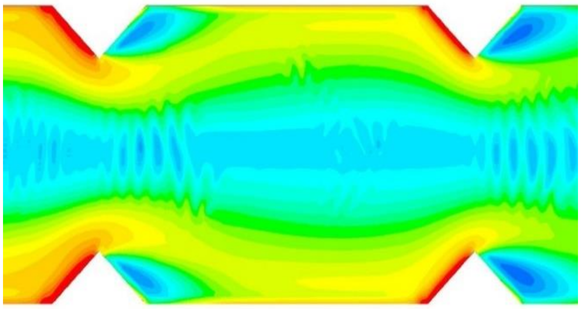

(c) Triangle ribbed duct

Fig. 13. Flow distribution of ribbed duct at 0.6 m/s water velocity and 0.18 m/s air velocity.

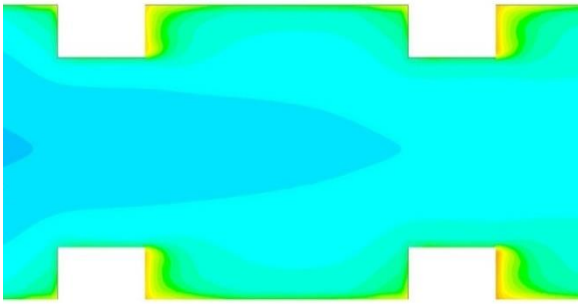

(a) Rectangular ribbed duct.

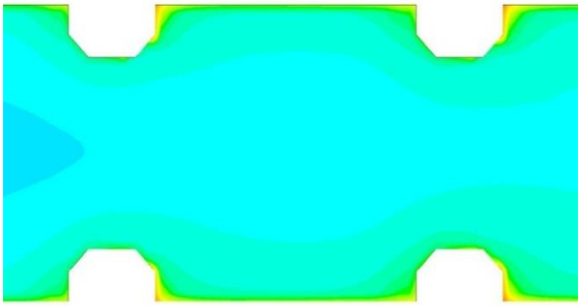

(b) Trapezoidal ribbed duct.

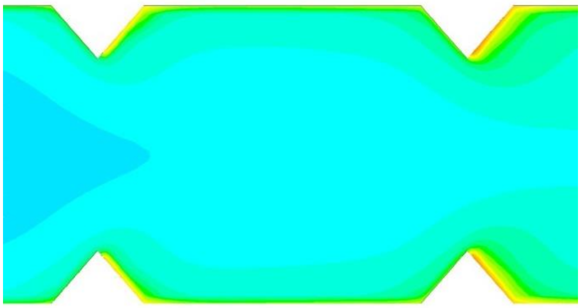

(c) Triangle ribbed duct.

Fig. 14. Temperature distribution of ribbed duct at 0.6 m/s water velocity and 0.18 m/s air velocity.

Nomenclature	
μ: Dynamic viscosity kg/m.s)	Re: Reynolds number (ρ u /μ)
b: Rib bitch distance (m)	T: Temperature (K)
cp: Specific heat (j/kg.K)	u: Velocity (m/s)
D: Diameter (m)	w: Rib base width (m)
e: Rib height (m)	x: Flow quality
F: Force (N)	X: Distance on the x axis
f: Friction	X_{TT}: Martinelli parameter
g: Gravity (m^2/s)	α: Volume fraction
h: Heat transfer coefficient ($w/m^2.K$)	ϵ: Turbulent dissipation rate (m^2/s^3)
k: Thermal conductivity (w/m.K)	ρ: Density (kg/m^3)
Nu: Nusselt number (h D/k)	σ: Surface tension (kg/m)
Pr: Prandtl number (μ cp/k)	
Subscript	
a: Air	L: Liquid
B: Bulk	m: Mixture
G: Gas	TP: Two phase
k: Phase	w: Wall, Water

References

[1] Ansari M. R., Gheisari R., and Azadi M., “Flow pattern change in horizontal rectangular laterally ribbed ducts through alteration of the ribs thickness and pitch”, *International Journal of Multiphase Flow*, vol. 54, pp. 11–21, 2013.

[2] Ansari M.R., and Arzandi B., “Two-phase gas–liquid flow regimes for smooth and ribbed rectangular ducts”, *International Journal of Multiphase Flow*, vol. 38, pp.118–125, 2012.

[3] Boukadoum A. B., and Benzaoui A., “CFD based analysis of heat transfer enhancement in solar air heater provided with transverse rectangular ribs", *Energy Procedia*, vol. 50, pp. 761-772, 2014.

[4] Boyko L. D., and Kruzhilin G. N., " Heat transfer and hydrolic resistance during condensation of steam in a horizontal tube and in a bundle of tubes", *Int. J. Heat Mass Transfer*, vol. 10, pp. 361-373, 1967.

[5] Coletti F., Jacono D. L., Cresci I., and Arts T., “Turbulent flow in rib-roughened channel under the effect of Coriolis and rotational buoyancy forces”, *Physics of Fluids*, vol. 26, 2014.

[6] Fluent User’s Guide, Modeling Multiphase Flows, Fluent Inc. September 29, 2006.

[7] Jaiswal S., and Aharwal K. R., “Three Dimensional CFD Analysis of Rectangular Roughened Channel”, *International Journal of Engineering Research & Technology (IJERT)*, vol. 4, Issue 06, June-2015.

[8] Kim D., “Improved Convective Heat Transfer Correlations for Two-Phase Two-Component Pipe Flow”, *KSME International Journal*, vol. 16, No.3, pp. 403- 422, 2002.

[9] Kim D., and Ghajar A. J., “Heat transfer measurements and correlations for air–water flow of different flow patterns in a horizontal pipe”, *Experimental Thermal and Fluid Science*, vol. 25, pp. 659–676, 2002.

[10] Komeil M. , Rohollah R., and Farhad T., “Effects of Rib Shapes on Heat Transfer Characteristics of Turbulent Flow of Al2O3-Water Nanofluid inside Ribbed Tubes”, *Iran. J. Chem. Chem. Eng*, vol. 34, No. 3, pp. 61-77, 2015.

[11] Manca O. , Nardini S., and Ricci D., “Numerical Study of Air Forced Convection in a Chanel Provided with Inclined Ribs”, *Frontiers in Heat and Mass Transfer (FHMT)*, 2011.

[12] Martin B. W., and Sims G. E., “Forced Convection Heat Transfer to Water with Air Injection in a Rectangular Duct”, *Int. J. Heat Mass Transfer*. vol. 14, pp. 1115-I 134., 1971.

[13] Mohan M. Vijay, “A STUDY OF HEAT TRANSFER IN TWO-PHASE TWO-COMPONENT FLOW IN A VERTICAL TUBE”, PhD. Eng. thesis, The University of Manitoba, Jan. 1999.

[14] Sánta R., “The Analysis of Two-Phase Condensation Heat Transfer Models Based on the Comparison of the Boundary Condition”, *Acta Polytechnica Hungarica*, vol. 9, No. 6, pp. 167-180, 2012.

[15] Serizawa A., Kataoka I., and Michiyoshi I., "Turbulence structure of air - water bubbly flow - III. Transport properties", *Int. J. Multiphase flow*, vol. 2, pp. 247-259, 1975.

[16] Sieder E. N., and Tate G. E. , “Heat Transfer and Pressure Drop of Liquids in Tubes”, *Ind. Eng. Chem*., vol. 28, No. 12, pp. 1429-1435, 1936.

[17] Song X.Q., Lin J.Z., Zhao J.F., and Shen T.Y., “Research on reducing erosion by adding ribs on the wall in particulate two-phase flows”, *Wear*, vol. 193, pp. 1-7, 1996.

[18] Yemenici O., and Sakin A., “Numerical Investigation of Heat Transfer for Laminar and Turbulent Flow over Ribbed Walls”, *International Journal of Engineering and Advanced Technology (IJEAT)*, vol. 2, pp. 163-166, Issue-6, August 2013.